Title

Subsurface Oxygen in Oxide-Derived Copper Electrocatalysts for Carbon Dioxide Reduction

Journal

The Journal of Physical Chemistry Letters, 8(1)

ISSN

1948-7185

Authors

Eilert, André

Cavalca, Filippo

Roberts, F Sloan

et al.

Publication Date

2017-01-05

DOI

10.1021/acs.jpclett.6b02273

Peer reviewed

Subsurface Oxygen in Oxide-Derived Copper Electrocatalysts for Carbon Dioxide Reduction

Journal:	*The Journal of Physical Chemistry Letters*
Manuscript ID	jz-2016-02273x.R2
Manuscript Type:	Letter
Date Submitted by the Author:	n/a
Complete List of Authors:	Eilert, André; SLAC National Accelerator Laboratory; Stanford University, SUNCAT Center for Interface Science and Catalysis, Department of Chemical Engineering; Stockholms Universitet, Department of Physics Cavalca, Filippo; SLAC National Accelerator Laboratory; Stanford University, SUNCAT Center for Interface Science and Catalysis, Department of Chemical Engineering; Stockholms Universitet, Department of Physics Roberts, Francis; SLAC National Accelerator Laboratory; Stanford University, SUNCAT Center for Interface Science and Catalysis, Department of Chemical Engineering; Stockholms Universitet, Department of Physics Osterwalder, Jürg; Universität Zürich, Physics Liu, Chang; Stockholms Universitet, Department of Physics Favaro, Marco; Lawrence Berkeley National Laboratory, Advanced Light Source (ALS) and Joint Center for Artificial Photosynthesis (JCAP) Crumlin, Ethan; E O Lawrence Berkeley National Laboratory, Advanced Light Source Ogasawara, Hirohito; SLAC National Accelerator LAboratory, Friebel, Daniel; SLAC National Accelerator Laboratory, Stanford Synchrotron Radiation Lightsource Pettersson, Lars; Stockholm University, Department of Physics Nilsson, Anders; SLAC National Accelerator Laboratory, SUNCAT crt for Interface Science and Catalysis; Stanford University, SUNCAT Center for Interface Science and Catalysis, Department of Chemical Engineering; Stockholms Universitet, Department of Physics

Subsurface Oxygen in Oxide-Derived Copper Electrocatalysts for Carbon Dioxide Reduction

André Eilert,[†,‡,∥] Filippo Cavalca,[†,‡,∥] F. Sloan Roberts,[†,‡,∥] Jürg Osterwalder,[§] Chang Liu,[∥] Marco Favaro,[⊥,||,ø] Ethan J. Crumlin,[⊥] Hirohito Ogasawara,[†] Daniel Friebel,[†] Lars G. M. Pettersson,[∥] and Anders Nilsson[,†,‡,∥]*

[†]SLAC National Accelerator Laboratory, 2575 Sand Hill Road, Menlo Park, California 94025, USA

[‡]SUNCAT Center for Interface Science and Catalysis, Department of Chemical Engineering, Stanford University, 443 Via Ortega, Stanford, California 95305, USA

[∥]Department of Physics, AlbaNova University Center, Stockholm University, S-10691 Stockholm, Sweden

[§]Department of Physics, University of Zürich, Winterthurerstrasse 190, 8057 Zürich, Switzerland

[⊥]Advanced Light Source, Lawrence Berkeley National Laboratory, 6 Cyclotron Road, Berkeley, California 94720, USA.

[||]Joint Center for Artificial Photosynthesis, Lawrence Berkeley National Laboratory, 1 Cyclotron Road, Berkeley, California 94720, USA.

[ø]Chemical Sciences Division, Lawrence Berkeley National Laboratory, 1 Cyclotron Road, Berkeley, California 94720, USA.

Corresponding Author

[*]Stockholm University, Chemical Physics, 10691 Stockholm, Sweden. Email: andersn@fysik.su.se.

ABSTRACT

Copper electrocatalysts derived from an oxide have shown extraordinary electrochemical properties for the carbon dioxide reduction reaction (CO_2RR). Using *in situ* Ambient Pressure X-ray Photoelectron Spectroscopy (APXPS) and quasi *in situ* Electron Energy Loss Spectroscopy (EELS) in a Transmission Electron Microscope (TEM), we show that there is a substantial amount of residual oxygen in nanostructured, oxide-derived copper electrocatalysts, but no residual copper oxide. Based on these findings in combination with Density Functional Theory (DFT) simulations, we propose that residual subsurface oxygen changes the electronic structure of the catalyst and creates sites with higher carbon monoxide binding energy. If such sites are stable under the strongly reducing conditions found in CO_2RR, these findings would explain the high efficiencies of oxide-derived copper in reducing carbon dioxide to multi-carbon compounds such as ethylene.

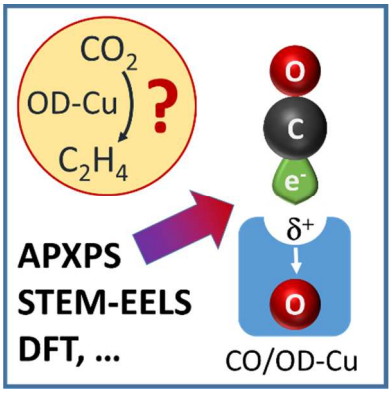

KEYWORDS In Situ, Ambient-Pressure X-Ray Photoelectron Spectroscopy, Scanning Transmission Electron Microscopy, Electron Energy Loss Spectroscopy, Density Functional Theory

A promising path towards a sustainable energy future with net-neutral CO_2 emissions is the combination of renewable electricity production with the electroreduction of carbon dioxide (CO_2RR), that needs a suitable electrocatalyst.[1,2] Among all pure metals, copper is the only one that gives a rich gamut of single- and multi-carbon products,[3–5] which can be explained by an optimal binding energy of CO to the surface.[6,7] However, the explanation becomes more complicated when dealing with nanostructured copper materials derived from oxidized precursors, which show both higher activity and greatly enhanced selectivity towards multi-carbon products.[8–16] It has been hypothesized that this could be related for instance to an increase of local pH,[17–19] grain boundaries,[20] undercoordinated sites,[21] or residual oxides.[22–24]

Several groups have shown the existence of sites with higher CO binding energy in oxide-derived copper.[23,25] However, if the increased binding energy is caused by a simple shift of the *d*-band in the catalyst (such as if we had nickel instead of copper), scaling relations would actually predict a higher overpotential for CO-CO-coupling on Cu(100).[7] Furthermore, an experimental study of different transition metals also suggests that an increase in CO binding energy actually lowers CO_2RR activity.[5] In contrast, if the increased binding energy has a different origin, such an understanding could become a future strategy to overcome scaling relations.

A polycrystalline copper foil was exposed to electrochemical oxidation-reduction cycles that increased the overall CO_2RR activity of the catalyst and improved the product yield towards more ethylene vs. methane (Figure S1). This change in activity and selectivity comes together with a pronounced change in the O 1*s* APXPS (Figure 1). The reported photoelectron spectra were measured *in situ*, i.e. in the chemical environment of a few nm thick layer of electrolyte (4 mM KCl in 0.1 M $KHCO_3$), immediately after pulling the sample out of the beaker (Figure S2).[26–28]

Figure 1*a* shows a spectrum of the pristine copper foil after four electrochemical reduction cycles, to remove surface oxides. The spectrum consists of a gas phase water peak at 536.2 eV apparent binding energy (yellow), a liquid water peak at 533.7 eV (red) and a third, adventitious oxygen peak at 531.7 eV (green). The intensity of the third (green) peak does not decrease upon further reduction as shown in Figure S3. Its origin is discussed below. Shifts induced by an electrochemical double-layer can be excluded due to the sufficiently high concentration of the electrolyte used.[29] The corresponding Cu $2p_{3/2}$ spectrum (Figure 2*a*) shows metallic copper. However, small contributions from Cu(I) cannot be excluded as Cu(I) compounds are typically shifted by only ca. 100 meV to lower binding energies with respect to metallic copper.[30]

After oxidation, the O 1*s* spectrum (Figure 1*b*) gains two components that can be assigned to $CuCO_3$/$Cu(OH)_2$ and Cu_2O, respectively.[30,31] Possible underlying intensity of the aforementioned adventitious oxygen peak at 531.7 eV cannot be resolved due to overlap with these components. The corresponding Cu $2p_{3/2}$ spectrum (Figure 2*b*) shows additional intensity at 934.6 eV which is in accordance with $CuCO_3$/$Cu(OH)_2$, whereas the Cu_2O fraction cannot be resolved due to the small shift of Cu(I) species. Scanning the Cl 2*p* spectral region did not show any significant intensity (Figure S4), proving the absence of CuCl compounds in spite of the presence of 4 mM chloride in the electrolyte (which is below the detection limit), which is in accordance with an earlier XAS study on a similar system.[9]

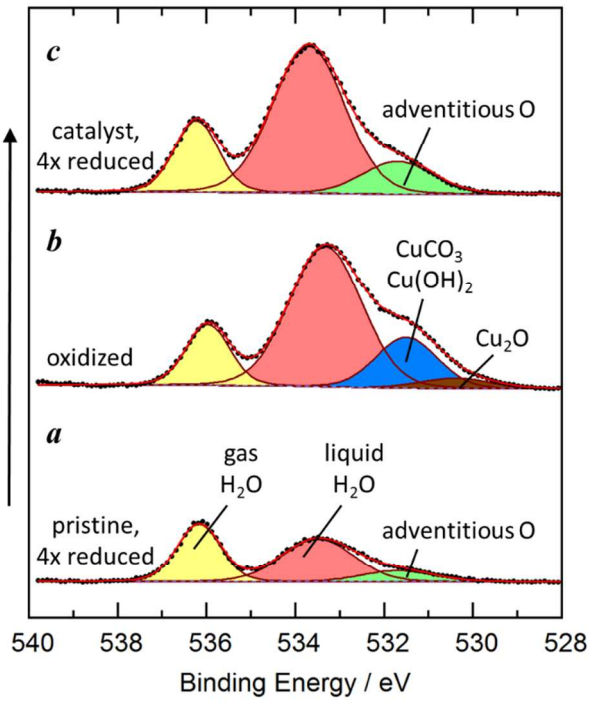

Figure 1. In situ O 1*s* APXPS spectra measured with an incident photon energy of 3996 eV. (a) Pristine sample. (b) Oxidation of the pristine sample leads to additional intensity at binding energies below 533 eV due to the formation of oxidized compounds such as $CuCO_3$, $Cu(OH)_2$ and Cu_2O. Furthermore, the liquid water peak increased indicating a thicker water overlayer. (c) The initially oxidized and then reduced sample contains significantly more adventitious oxygen (green) than the pristine sample before oxidation. Intensities not normalized.

After reduction, the O 1*s* spectrum (Figure 1*c*) shows a substantially increased adventitious component at 531.7 eV (green), compared to the initial spectrum before oxidation. Furthermore, the oxidized and reduced samples give rise to an increased amount of liquid water on the sample, visible both by an increased liquid water peak in the O 1*s* spectrum and by a stronger attenuation of the Cu 2*p* line. This behavior was reproducible and not an effect of the background pressure of water vapor which was slightly lower for the oxidized and reduced samples, compared to the

pristine one. The fact that the oxidized and reduced samples show a similar moist content (which is significantly higher than for the pristine sample) points away from surface polarity being the main cause of this effect. It is likely that mainly nano-structuring of the sample surface (Figure S5) causes the increased hydrophilicity.

For quantification of the relative increase of adventitious oxygen, attenuation by the water overlayer has to be considered. Figure S6 describes different normalization schemes which are based on different assumptions. As a result, the increase of adventitious oxygen after oxidation and four subsequent reduction cycles can be estimated to be in the order of a factor 10.

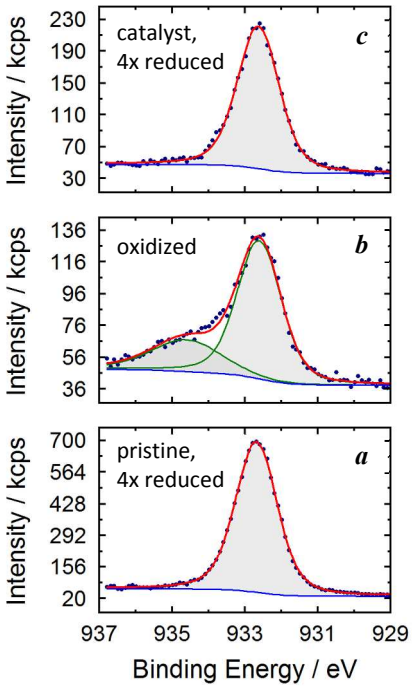

Figure 2. *In situ* Cu $2p_{3/2}$ APXPS spectra. Spectra of the reduced sample (*a*, *c*) do not contain any Cu(II). The oxidized spectrum (*b*) shows an additional Cu(II) component such as malachite ($CuCO_3/Cu(OH)_2$).

We also observed K 2*p* intensity and additional C 1*s* intensity at 289 eV (Figure S7) sporadically associated with samples, which roughly scaled with each other. This indicates that the electrolyte contributes to the adventitious (green) oxygen component in the O 1*s* spectrum (Figure 1), especially since the O 1*s* binding energy of carbonate is centered at about 531.7 eV.[30] However, whereas a strong correlation between adventitious oxygen and sample history is present (*i.e.* whether it was pre-oxidized or not), the correlation between K 2*p* and adventitious O 1*s* intensity is rather weak, giving rise to the conclusion that the adventitious oxygen signal is not solely caused by electrolyte. Furthermore, potential dependent XPS using the dip-and-pull method[26,27] show that potassium is electronically not connected to the Cu working electrode (observable by a potential-dependent shift in apparent binding energy), whereas the best fit indicates that the adventitious oxygen component is mostly pinned to the Cu working electrode (Figure S8). This supports the hypothesis that an additional species, which is electronically connected to the working electrode, contributes to the adventitious (green) component in the O 1*s* spectrum (Figure 1). The appearance of electrolyte in the spectra is further discussed in the Supporting information.

Recently, the existence of residual Cu_2O in copper catalysts for CO_2RR was discussed.[23,24] However, the additional (green) peak at 531.7 eV in the O 1*s* spectrum cannot be caused by Cu_2O which would have been observed at 530.4 eV (compare to Figure 1*b*). Furthermore, Cu(II) components can be excluded by the Cu $2p_{3/2}$ spectrum (Figure 2*c*) that shows no peak at high binding energies. Other imaginable Cu(I) components, such as the hypothetical Cu(OH) or Cu_2CO_3, are generally not stable,[32] but cannot entirely be excluded.

It is a reasonable hypothesis that subsurface oxygen contributes to the additional (green) spectral component in Figure 1*c*, overlapping with the aforementioned electrolyte contribution. Also a contribution from specifically adsorbed HCO_3^-, supported by subsurface oxygen, is

imaginable. The inelastic mean free path of O 1*s* photoelectrons at a kinetic energy of 3470 eV in metallic copper is 3.9 nm.[33] Since the attenuation of photoelectrons follows an exponential decay with increasing depth, the majority of the observed signal stems from the top few nanometers of the catalyst. From a theoretical point of view, Korzhavyi and Sandström have calculated the trapping barriers of oxygen and OH^- in a monovacancy of Cu as 0.95 and 1.23 eV, respectively, and excluded water formation in this site, which points to the fact that oxygen could indeed be stable in certain subsurface sites in an aqueous environment and in the presence of hydrogen.[34]

Bluhm and co-workers have found an XPS spectroscopic signature of subsurface oxygen earlier in a copper catalyst for methanol oxidation.[35] In their study, peak assignments are tentative due to the challenging interpretation of data with many components and limited signal-to-noise ratio at high photon energies. Our Density Functional Theory (DFT) calculations suggest a relative difference of XPS binding energy between subsurface and surface oxygen of 0.8-1.7 eV (Table S2). Together with the known XPS binding energy of surface oxygen of ca. 530 eV,[36] it is consistent with the hypothesis that subsurface oxygen contributes to the additional spectral component at 531.7 eV. This is also in accordance with the silver-oxygen system that shows subsurface oxygen shifted towards higher XPS binding energy compared to surface oxygen.[37]

This conclusion is further backed by quasi *in situ* oxygen K-edge Electron Energy Loss Spectra (EELS) of a copper nanoparticle catalyst in a Transmission Electron Microscope (TEM) (Figure 3). In this experiment, electrochemical modifications and electrolyte removal by rinsing in water were performed in a protective nitrogen atmosphere outside the microscope, followed by sample transfer into the microscope using a vacuum transfer holder. Due to this experimental scheme, the sample was never in contact with air during the experiment. Figure 3*a* shows the oxidized sample with an EELS signature resembling that of Cu_2O.[38–40] Experimental details were

slightly different between EELS and APXPS (nanoparticles versus foil and lower pH in EELS), resulting in Cu_2O being the dominant species in EELS. After reduction, two chemically different oxygen species were found: one inside the catalyst, assignable to subsurface oxygen (*b*) and one in a precipitate on the surface of the catalyst (*c*). The precipitate contains K, C and O (Figure S9) and could be related to K_2CO_3 precipitation; more details can be found in the Supporting information, section 'Appearance of electrolyte in the APXPS spectra'. Both spectra (*b*) and (*c*) in Figure 3 exhibit a different line shape and a shift of +3.2 and +3.5 eV with respect to spectrum (*a*), respectively. This gives clear evidence for the changed chemical environment of subsurface oxygen with respect to Cu_2O. The energy shift of the oxygen K edge to higher energy losses in the reduced sample (*b*) compared to the oxidized one (*a*) is consistent with that observed in the O 1*s* APXPS (Figure 1), where adventitious oxygen (green) was found at ca. 1.3 eV higher binding energy than Cu_2O (brown). The different values for the energy shift between EELS and APXPS are caused by the non-metallic nature of the oxidized sample, that does not allow metallic screening in the APXPS of Cu_2O.[41] However, the similar shifts in Figs. 3*b* and (*c*) support the modelling of adventitious oxygen in APXPS by one peak (Figure 1, green component). Copper L-edge EELS spectra of the oxidized and reduced catalyst confirm Cu_2O and metallic copper, respectively (Figure S11).

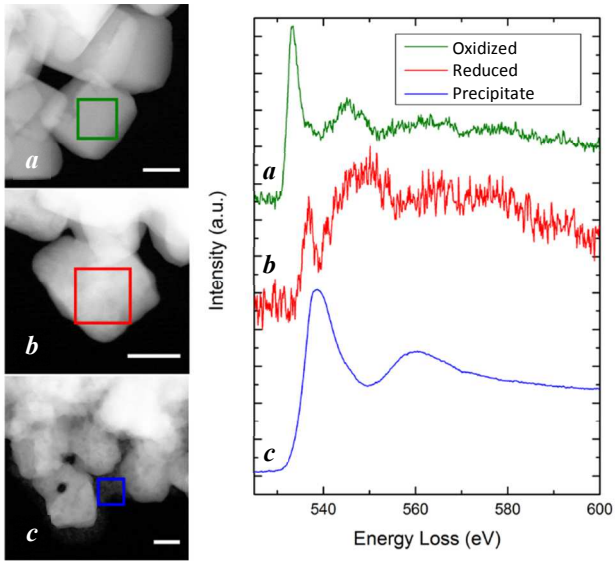

Figure 3. Scanning TEM annular dark field (ADF) images (left) and oxygen K EEL spectra (right) obtained in a quasi *in situ* TEM experiment mimicking the APXPS experiment. *a*) Oxidized sample: spectroscopic EELS signature of Cu_2O; *b*,*c*) reduced sample, *b*) EELS from a particle and *c*) EELS from the precipitate. Scale bars in the TEM images correspond to 30 nm. Squares in the TEM images depict the scanned areas for EELS. Edge shifts match qualitatively with APXPS binding energy shifts.

Recently, Lee *et al.*[23] and Mistry *et al.*[24] proposed residual Cu_2O after reduction that would explain the enhanced selectivity of oxide-derived Cu. Their *in situ* XANES data are consistent with a similar study by Eilert *et al.*[9] and an *in situ* Raman spectroscopy study by Ren *et al.*,[11] that showed a pure metallic phase after holding the sample at reductive potentials, but their *ex situ* TEM work that occurred after long exposure to air and *post mortem* sample preparation showed the presence of an oxide phase (a reference sample reduced with H_2 indicated that the oxide phase was not solely caused by exposure to air). However, in the present study our APXPS experiment was carried out *in situ* and our TEM experiment in a quasi *in situ* environment

without exposure to air and shows that there are no residual oxides but a pure metallic phase with a small amount of subsurface oxygen.

It is worth noting the difference between residual copper oxides such as Cu_2O or $Cu(OH)_2$ and trapped subsurface oxygen or OH^-. Since the catalyst is formed by reducing an oxidized Cu sample, it is supposed that subsurface oxygen is still in a negative oxidation state, which is compensated by polarization of the conduction electrons in the surrounding, mostly metallic copper atoms. This leads to substantially different properties and crystal structure compared to the oxide phase, which contains Cu in an oxidation state +I or +II.

CO bonding on late transition metals such as copper is governed by an interplay between π-bonding and σ-repulsion.[42–44] Both depend on the *d*-band position, however, the σ-repulsion is also sensitive to the occupancy of the Cu *sp*-band. Thus an electron acceptor which withdraws charge from the *sp*-band can reduce the repulsion as shown by Xin *et al*. for the case 2O-CO/Ru(0001).[45] In particular the free energy at elongated distances in comparison to the equilibrium position is affected.[45]

As an example, the influence of subsurface oxygen on the binding energy of CO on a Cu(100) surface was investigated by DFT. The CO binding energy was calculated for clean Cu(100) and for Cu(100) with an oxygen atom placed in interstitial sites in different layers below the surface (Table S3). Significant CO binding energy enhancement is observed for oxygen atom implantations down to the 3rd subsurface layer.

Hence, we find that the interaction of the subsurface oxygen atom with the metal causes an increased CO binding energy (Figure S12). A larger CO binding energy could lead to a higher CO coverage of the catalyst, which kinetically favors C-C-coupling over hydrogenation. There can be additional effects in the C-C coupling at longer CO-metal distances when electrolyte and water are present since the oxygen-induced changes minimize the σ-repulsion from the more

spatially extended *sp*-band wave functions.[45] This could solve the apparent contradiction between studies by Ma *et al.*[7] and Kuhl *et al.*[5] on the one side, which propose (on the basis of *d*-band scaling relations) no improved catalytic properties for catalysts with higher CO binding energy compared to clean Cu, and studies by Lee *et al.*[23] and Verdaguer-Casadevall *et al.*,[25] which show sites with an increased CO binding energy in oxide-derived Cu. The question is, however, whether subsurface oxygen could be stable close to the surface under such reducing conditions and if so it would be expected to require some unique sites created in the nanostructured system upon reduction of the oxide precursor. This question could be addressed by XPS with lower kinetic energy and by TEM with higher resolution and without precipitate.

The recent enhanced CO_2 selectivity correlation to grain boundaries in vapor deposited Cu on carbon nanotubes[20] could also be due to subsurface oxygen since the samples were exposed to air prior to the electrocatalytic measurements. Similarly the enhanced CO adsorption energy on reduced oxide-derived Cu is correlated to the amount of grain boundaries.[25] This could point to the fact that subsurface oxygen could preferentially be more stable and enhancing the reactivity of Cu metallic sites at grain boundaries.

Several studies have shown a preference for C-C-coupling on Cu(100) facets[8,46] and Li *et al*. proposed a break in scaling relations, caused by the stabilization of $*C_2O_2$ on the particular surface geometry of Cu(100).[47] Furthermore, it was shown that an increased local pH, caused by the consumption of protons in the pores of a rough catalyst, also promotes C-C-coupling.[17,18] However, studies which investigated those effects particularly for oxide-derived copper came to the conclusion, that neither the exposed facets[15] nor the increase in local pH[19] can sufficiently explain the extraordinary properties of these catalysts. An increased CO binding energy due to subsurface oxygen can thus be the crucial puzzle piece which makes oxide-derived copper so special for CO_2 reduction.

In conclusion, we have shown by *in situ* APXPS and quasi *in situ* EELS a correlation between favorable electrochemical properties of an oxide-derived copper catalyst for the electrochemical reduction of carbon dioxide, such as higher activity and higher yields of ethylene versus methane formation, and the existence of subsurface oxygen which is formed by oxidation-reduction cycles. Both APXPS and EELS prove the absence of residual copper oxide in the reduced electrocatalyst. We propose a mechanism in which subsurface oxygen increases the CO binding energy to the catalyst by reducing the σ-repulsion. This mechanism kinetically favors C-C-bond formation due to a higher CO coverage on the catalyst. However, this could only occur if some special sites in the near-surface region sufficiently inhibit diffusion to the first layer where oxygen would subsequently be protonated to water. This finding provides further insight on the "oxide-derived copper story" as it contributes to the explanation of the outstanding change in electrochemical properties due to oxidation and reduction of copper.

ASSOCIATED CONTENT

Supporting Information.

The Supporting Information is available free of charge.

Spectra, illustrations, detailed discussions of side aspects, experimental and computational details (PDF)

AUTHOR INFORMATION

Notes

The authors declare no competing financial interests.

ACKNOWLEDGMENT

This work was supported by the Air Force Office of Scientific Research through the MURI program under AFOSR Award No. FA9550-10-1-0572 and the Global Climate Energy Project at Stanford University. Ambient Pressure X-Ray Photoelectron Spectroscopy (APXPS) was performed at beamline 9.3.1 at Advanced Light Source. The Advanced Light Source is supported by the Director, Office of Science, Office of Basic Energy Sciences, of the U.S. Department of Energy under Contract No. DE-AC02-05CH11231. Scanning Electron Microscopy (SEM) and Transmission Electron Microscopy (TEM) were performed at Stanford Nano Shared Facilities (SNSF). We thank Fischione for providing the TEM vacuum transfer holder. Density Functional Theory (DFT) calculations were supported by the Knut and Alice Wallenberg (KAW) Foundation and the Swedish Energimyndigheten. CPU time was provided by the Swedish National Infrastructure for Computing (SNIC) at the HP2CN center. JO acknowledges financial support from the Stanford Institute for Materials and Energy Sciences (SIMES) and from the Swiss National Science Foundation. MF acknowledges Office of Science, Office of Basic Energy Science (BES), of the U.S. Department of Energy (DOE) under award no. DE-SC0004993 to the Joint Center for Artificial Photosynthesis (JCAP).

REFERENCES

(1) Lewis, N. S.; Nocera, D. G. Powering the Planet: Chemical Challenges in Solar Energy Utilization. *Proc. Natl. Acad. Sci. U. S. A.* **2006**, *103*, 15729–15735.

(2) Gattrell, M.; Gupta, N.; Co, A. Electrochemical Reduction of CO_2 to Hydrocarbons to Store Renewable Electrical Energy and Upgrade Biogas. *Energy Convers. Manag.* **2007**, *48*, 1255–1265.

(3) Hori, Y. Electrochemical CO2 Reduction on Metal Electrodes. In *Modern Aspects of Electrochemistry*; Springer, 2008; pp 89–189.

(4) Kuhl, K. P.; Cave, E. R.; Abram, D. N.; Jaramillo, T. F. New Insights into the Electrochemical Reduction of Carbon Dioxide on Metallic Copper Surfaces. *Energy Environ. Sci.* **2012**, *5*, 7050–7059.

(5) Kuhl, K. P.; Hatsukade, T.; Cave, E. R.; Abram, D. N.; Kibsgaard, J.; Jaramillo, T. F. Electrocatalytic Conversion of Carbon Dioxide to Methane and Methanol on Transition Metal Surfaces. *J. Am. Chem. Soc.* **2014**, *136*, 14107–14113.

(6) Peterson, A. A.; Nørskov, J. K. Activity Descriptors for CO_2 Electroreduction to Methane on Transition-Metal Catalysts. *J. Phys. Chem. Lett.* **2012**, *3*, 251–258.

(7) Ma, X.; Li, Z.; Achenie, L. E. K.; Xin, H. Machine-Learning-Augmented Chemisorption Model for CO_2 Electroreduction Catalyst Screening. *J. Phys. Chem. Lett.* **2015**, *6*, 3528–3533.

(8) Roberts, F. S.; Kuhl, K. P.; Nilsson, A. High Selectivity for Ethylene from Carbon Dioxide Reduction over Copper Nanocube Electrocatalysts. *Angew. Chem. Int. Ed.* **2015**, *54*, 5179–5182.

(9) Eilert, A.; Roberts, F. S.; Friebel, D.; Nilsson, A. Formation of Copper Catalysts for CO_2 Reduction with High Ethylene/Methane Product Ratio Investigated with in Situ X-Ray Absorption Spectroscopy. *J. Phys. Chem. Lett.* **2016**, *7*, 1466–1470.

(10) Li, C. W.; Ciston, J.; Kanan, M. W. Electroreduction of Carbon Monoxide to Liquid Fuel on Oxide-Derived Nanocrystalline Copper. *Nature* **2014**, *508*, 504–507.

(11) Ren, D.; Deng, Y.; Handoko, A. D.; Chen, C. S.; Malkhandi, S.; Yeo, B. S. Selective Electrochemical Reduction of Carbon Dioxide to Ethylene and Ethanol on copper(I) Oxide Catalysts. *ACS Catal.* **2015**, *5*, 2814–2821.

(12) Raciti, D.; Livi, K. J.; Wang, C. Highly Dense Cu Nanowires for Low-Overpotential CO_2 Reduction. *Nano Lett.* **2015**, *15*, 6829–6835.

(13) Ma, M.; Djanashvili, K.; Smith, W. A. Selective Electrochemical Reduction of CO_2 to CO on CuO-Derived Cu Nanowires. *Phys. Chem. Chem. Phys.* **2015**, *17*, 20861–20867.

(14) Chi, D.; Yang, H.; Du, Y.; Lv, T.; Sui, G.; Wang, H.; Lu, J. Morphology-Controlled CuO Nanoparticles for Electroreduction of CO_2 to Ethanol. *RSC Adv.* **2014**, *4*, 37329–37332.

(15) Kas, R.; Kortlever, R.; Milbrat, A.; Koper, M. T. M.; Mul, G.; Baltrusaitis, J. Electrochemical CO_2 Reduction on Cu_2O-Derived Copper Nanoparticles: Controlling the Catalytic Selectivity of Hydrocarbons. *Phys. Chem. Chem. Phys.* **2014**, *16*, 12194–12201.

(16) Dutta, A.; Rahaman, M.; Luedi, N. C.; Mohos, M.; Broekmann, P. Morphology Matters: Tuning the Product Distribution of CO_2 Electroreduction on Oxide-Derived Cu Foam Catalysts. *ACS Catal.* **2016**, *6*, 3804–3814.

(17) Gupta, N.; Gattrell, M.; MacDougall, B. Calculation for the Cathode Surface Concentrations in the Electrochemical Reduction of CO_2 in $KHCO_3$ Solutions. *J. Appl. Electrochem.* **2006**, *36*, 161–172.

(18) Varela, A. S.; Kroschel, M.; Reier, T.; Strasser, P. Controlling the Selectivity of CO_2 Electroreduction on Copper: The Effect of the Electrolyte Concentration and the Importance of the Local pH. *Catal. Today* **2016**, *260*, 8–13.

(19) Roberts, F. S.; Kuhl, K. P.; Nilsson, A. Electroreduction of Carbon Monoxide over a Copper Nanocube Catalyst: Surface Structure and pH Dependence on Selectivity. *ChemCatChem* **2016**, *8*, 1119–1124.

(20) Feng, X.; Jiang, K.; Fan, S.; Kanan, M. W. A Direct Grain-Boundary-Activity Correlation for CO Electroreduction on Cu Nanoparticles. *ACS Cent. Sci.* **2016**, *2*, 169–174.

(21) Tang, W.; Peterson, A. A.; Varela, A. S.; Jovanov, Z. P.; Bech, L.; Durand, W. J.; Dahl, S.; Nørskov, J. K.; Chorkendorff, I. The Importance of Surface Morphology in Controlling the Selectivity of Polycrystalline Copper for CO_2 Electroreduction. *Phys. Chem. Chem. Phys.* **2012**, *14*, 76–81.

(22) Kim, D.; Lee, S.; Ocon, J. D.; Jeong, B.; Lee, J. K.; Lee, J. Insights into an Autonomously Formed Oxygen-Evacuated Cu_2O Electrode for the Selective Production of C_2H_4 from CO_2. *Phys. Chem. Chem. Phys.* **2014**, *17*, 824–830.

(23) Lee, S.; Kim, D.; Lee, J. Electrocatalytic Production of C3-C4 Compounds by Conversion of CO_2 on a Chloride-Induced Bi-Phasic Cu_2O-Cu Catalyst. *Angew. Chem. Int. Ed.* **2015**, *127*, 14914–14918.

(24) Mistry, H.; Varela, A. S.; Bonifacio, C. S.; Zegkinoglou, I.; Sinev, I.; Choi, Y.-W.; Kisslinger, K.; Stach, E. A.; Yang, J. C.; Strasser, P.; et al. Highly Selective Plasma-Activated Copper Catalysts for Carbon Dioxide Reduction to Ethylene. *Nat. Commun.* **2016**, *7*, 12123.

(25) Verdaguer-Casadevall, A.; Li, C. W.; Johansson, T. P.; Scott, S. B.; McKeown, J. T.; Kumar, M.; Stephens, I. E. L.; Kanan, M. W.; Chorkendorff, I. Probing the Active Surface Sites for CO Reduction on Oxide-Derived Copper Electrocatalysts. *J. Am. Chem. Soc.* **2015**, *137*, 9808–9811.

(26) Axnanda, S.; Crumlin, E. J.; Mao, B.; Rani, S.; Chang, R.; Karlsson, P. G.; Edwards, M. O. M.; Lundqvist, M.; Moberg, R.; Ross, P.; et al. Using "tender" X-Ray Ambient Pressure X-Ray Photoelectron Spectroscopy as a Direct Probe of Solid-Liquid Interface. *Sci. Rep.* **2015**, *5*, 9788.

(27) Ali-Löytty, H.; Louie, M. W.; Singh, M. R.; Li, L.; Sanchez Casalongue, H. G.; Ogasawara, H.; Crumlin, E. J.; Liu, Z.; Bell, A. T.; Nilsson, A.; et al. Ambient-Pressure XPS Study of a Ni–Fe Electrocatalyst for the Oxygen Evolution Reaction. *J. Phys. Chem. C* **2016**, *120*, 2247–2253.

(28) Crumlin, E. J.; Bluhm, H.; Liu, Z. In Situ Investigation of Electrochemical Devices Using Ambient Pressure Photoelectron Spectroscopy. *J. Electron Spectrosc. Relat. Phenom.* **2013**, *190*, *Part A*, 84–92.

(29) Favaro, M.; Jeong, B.; Ross, P. N.; Yano, J.; Hussain, Z.; Liu, Z.; Crumlin, E. J. Unravelling the Electrochemical Double Layer by Direct Probing of the Solid/Liquid Interface. *Nat. Commun.* **2016**, *7*, 12695.

(30) NIST X-ray Photoelectron Spectroscopy Database, Version 4.1 (National Institute of Standards and Technology, Gaithersburg, 2012); http://srdata.nist.gov/xps/.

(31) Svintsitskiy, D. A.; Stadnichenko, A. I.; Demidov, D. V.; Koscheev, S. V.; Boronin, A. I. Investigation of Oxygen States and Reactivities on a Nanostructured Cupric Oxide Surface. *Appl. Surf. Sci.* **2011**, *257*, 8542–8549.

(32) Massey, A. G. 27. - COPPER. In *The Chemistry of Copper, Silver and Gold*; Pergamon Texts in Inorganic Chemistry; Pergamon, 1973; pp 1–78.

(33) Da, B.; Shinotsuka, H.; Yoshikawa, H.; Ding, Z. J.; Tanuma, S. Extended Mermin Method for Calculating the Electron Inelastic Mean Free Path. *Phys. Rev. Lett.* **2014**, *113*.

(34) Korzhavyi, P. A.; Sandström, R. Monovacancy in Copper: Trapping Efficiency for Hydrogen and Oxygen Impurities. *Comput. Mater. Sci.* **2014**, *84*, 122–128.

(35) Bluhm, H.; Hävecker, M.; Knop-Gericke, A.; Kleimenov, E.; Schlögl, R.; Teschner, D.; Bukhtiyarov, V. I.; Ogletree, D. F.; Salmeron, M. Methanol Oxidation on a Copper Catalyst Investigated Using in Situ X-Ray Photoelectron Spectroscopy. *J. Phys. Chem. B* **2004**, *108*, 14340–14347.

(36) Tillborg, H.; Nilsson, A.; Hernnäs, B.; Mårtensson, N. O/Cu(100) Studied by Core Level Spectroscopy. *Surf. Sci.* **1992**, *269*, 300–304.

(37) Rocha, T. C. R.; Oestereich, A.; Demidov, D. V.; Hävecker, M.; Zafeiratos, S.; Weinberg, G.; Bukhtiyarov, V. I.; Knop-Gericke, A.; Schlögl, R. The Silver–oxygen System in

Catalysis: New Insights by near Ambient Pressure X-Ray Photoelectron Spectroscopy. *Phys. Chem. Chem. Phys.* **2012**, *14*, 4554–4564.

(38) Cavalca, F.; Laursen, A. B.; Wagner, J. B.; Damsgaard, C. D.; Chorkendorff, I.; Hansen, T. W. Light-Induced Reduction of Cuprous Oxide in an Environmental Transmission Electron Microscope. *ChemCatChem* **2013**, *5*, 2667–2672.

(39) Hävecker, M.; Knop-Gericke, A.; Schedel-Niedrig, T.; Schlögl, R. High-Pressure Soft X-Ray Absorption Spectroscopy: A Contribution to Overcoming the "pressure Gap" in the Study of Heterogeneous Catalytic Processes. *Angew. Chem. Int. Ed.* **1998**, *37*, 1939–1942.

(40) Grioni, M.; Van Acker, J. F.; Czyžyk, M. T.; Fuggle, J. C. Unoccupied Electronic Structure and Core-Hole Effects in the X-Ray-Absorption Spectra of Cu_2O. *Phys. Rev. B* **1992**, *45*, 3309.

(41) Nilsson, A. Applications of Core Level Spectroscopy to Adsorbates. *J. Electron Spectrosc. Relat. Phenom.* **2002**, *126*, 3–42.

(42) Föhlisch, A.; Nyberg, M.; Bennich, P.; Triguero, L.; Hasselström, J.; Karis, O.; Pettersson, L. G. M.; Nilsson, A. The Bonding of CO to Metal Surfaces. *J. Chem. Phys.* **2000**, *112*, 1946–1958.

(43) Pettersson, L. G. M.; Nilsson, A. A Molecular Perspective on the D-Band Model: Synergy between Experiment and Theory. *Top. Catal.* **2014**, *57*, 2–13.

(44) Nilsson, A.; Pettersson, L. G.; Nørskov, J. *Chemical Bonding at Surfaces and Interfaces*; Elsevier, 2011.

(45) Xin, H.; LaRue, J.; Öberg, H.; Beye, M.; Dell'Angela, M.; Turner, J. J.; Gladh, J.; Ng, M. L.; Sellberg, J. A.; Kaya, S.; et al. Strong Influence of Coadsorbate Interaction on CO Desorption Dynamics on Ru(0001) Probed by Ultrafast X-Ray Spectroscopy and *Ab Initio* Simulations. *Phys. Rev. Lett.* **2015**, *114*.

(46) Schouten, K. J. P.; Qin, Z.; Gallent, E. P.; Koper, M. T. M. Two Pathways for the Formation of Ethylene in CO Reduction on Single-Crystal Copper Electrodes. *J. Am. Chem. Soc.* **2012**, *134*, 9864–9867.

(47) Li, H.; Li, Y.; Koper, M. T. M.; Calle-Vallejo, F. Bond-Making and Breaking between Carbon, Nitrogen, and Oxygen in Electrocatalysis. *J. Am. Chem. Soc.* **2014**, *136*, 15694–15701.